

See discussions, stats, and author profiles for this publication at: <https://www.researchgate.net/publication/265646966>

# Surface Modification of ITO Nanoparticles by Trimesic Acid: A Combined Experimental and DFT Study

ARTICLE in THE JOURNAL OF PHYSICAL CHEMISTRY C · AUGUST 2014

Impact Factor: 4.77 · DOI: 10.1021/jp5063447

CITATIONS

2

READS

6

7 AUTHORS, INCLUDING:



Zhangxian Chen

National University of Singapore

13 PUBLICATIONS 123 CITATIONS

SEE PROFILE



Liang Huang

University of Wyoming

14 PUBLICATIONS 21 CITATIONS

SEE PROFILE



Hansong Cheng

China University of Geosciences

166 PUBLICATIONS 2,408 CITATIONS

SEE PROFILE

# Surface Modification of ITO Nanoparticles by Trimesic Acid: A Combined Experimental and DFT Study

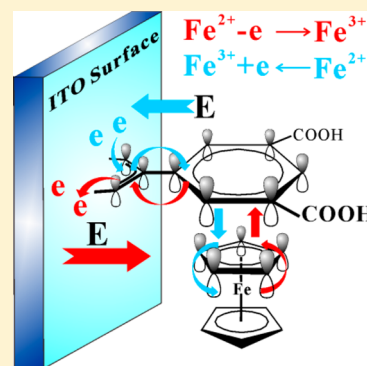
Zhangxian Chen,<sup>†</sup> Qingfan Zhang,<sup>‡</sup> Liang Huang,<sup>†,‡</sup> Ran Li,<sup>†</sup> Wanchao Li,<sup>†</sup> Guoqin Xu,<sup>\*,†</sup> and Hansong Cheng<sup>\*,†,‡</sup>

<sup>†</sup>Department of Chemistry, National University of Singapore, 3 Science Drive 3, Singapore 117543

<sup>‡</sup>Sustainable Energy Laboratory, China University of Geosciences Wuhan, 388 Lumo Road, Wuhan, China 430074

## S Supporting Information

**ABSTRACT:** Surface modification of ITO films is important for their applications in optoelectronics. Herein, trimesic acid was used to modify polycrystalline ITO nanoparticles. Spectroscopic results indicate the formation of carboxylate on the ITO nanoparticle surfaces upon modification. Density functional theory calculations reveal an upstanding adsorption structure of the acid molecule on the ITO (111) surface and the formation of a carboxylate surface species. The dissociative chemisorption of trimesic acid on the selected surface was found to be thermodynamically exothermic and kinetically facile. We show that the surface-modified ITO nanoparticles are capable of effectively enhancing the charge-transfer rate and substantially boosting electrocatalytic effect toward redox of ferrocene via a  $\pi$ - $\pi$  interaction between ferrocene and the adsorbate.



## ■ INTRODUCTION

As an industry workhorse, Sn-doped indium oxide (ITO) thin films have been widely utilized in various optoelectronic devices as transparently conductive media, which can now be routinely fabricated with a variety of techniques, most prominently high vacuum sputtering and solution processes.<sup>1,2</sup> Surface modifications of ITO thin films are deemed highly desirable since they can effectively tune the wettability of the films to organic layers and thus effectively enhance charge transfer rates across interfaces, e.g., the interface between ITO films and PEDOT:PSS.<sup>3,4</sup> Efficient surface modification tailored for specific applications is imperative to achieve high performance of electronic devices, such as organic photovoltaics and organic light-emitting devices.

Most surface modifications for ITO films are realized with organic phosphonic acids and silanes, owing to the strong capability of these molecules to form covalent bonds with metal-oxide surfaces via various dentate binding modes or O-Si-O linkages.<sup>3,5</sup> To date, only few carboxylic acids have been used for surface modifications of ITO films, such as 3-thiophene acetic acid, ferrocene dicarboxylic acid, and other ferrocene-based carboxylic acids,<sup>4,6-8</sup> since these molecules could offer the advantage to allow simple electrochemical characterizations or further modifications via carefully designed chemical processes upon adsorption. Although the adsorption of these acids has been thoroughly characterized by various experimental techniques,<sup>4,6,7</sup> the interactions between acid molecules and ITO surfaces have not been well-understood largely due to the complexity of the polycrystalline surfaces of ITO films. The driving forces that dictate the adsorption are

deemed to be electrostatic, hydrogen bonding, and coordinate-covalent bonding between carboxylate and metal ion sites either individually or collectively.<sup>3</sup> A judicious choice of carboxylic acids for a targeted application requires mechanistic understanding of the nature of the interactive force that governs the surface modification. Trimesic acid (TMA) differs significantly from these carboxylic acids that have been utilized for ITO surface modifications. The molecule is potentially capable of tuning the surface chemistry of ITO films differently via its extensive  $\pi$ -conjugation and thus enabling new ways of ITO surface modification for electronic devices.

Most surface modifications of ITO films by carboxylic acids were conducted through the adsorption of acid molecules on vacuum-deposited ITO thin films.<sup>3,4,6-8</sup> To date, a direct modification of ITO nanoparticles by carboxylic acids has not been reported to our knowledge. A direct surface modification of ITO nanoparticles offers significant advantages over postdeposition modification, such as more complete surface modification, easier nanoparticle dispersion by choosing an appropriate surface modifier, and more facile deposition for printed electronics.<sup>9</sup>

In this Article, we report a combined experimental and theoretical study on direct surface modification of ITO nanoparticles by trimesic acid. The surface chemistry and chemical bonding upon TMA modification have been systematically characterized by spectroscopic techniques and analyzed

Received: June 26, 2014

Revised: August 15, 2014

Published: August 18, 2014



on the basis of density functional theory (DFT) calculations. It is shown that the TMA molecules undergo quasidissociative chemisorption upon adsorption on ITO nanoparticles, forming carboxylate species with strong covalent bonds with ITO surfaces. Ferrocene was chosen as the electrochemical probe to detect the electrocatalytic effect of ITO nanoparticles toward its redox reaction. A remarkable enhancement of electrocatalytic capability upon ITO nanoparticle modification was demonstrated. A  $\pi$ - $\pi$  interaction between the adsorbate and ferrocene was found to be responsible for the substantially enhanced electrocatalytic capability.

## ■ EXPERIMENTAL AND COMPUTATIONAL DETAILS

**Surface Modification by Trimesic Acid.** ITO nanoparticles (dopant ratio = 10 wt %) were synthesized via a coprecipitation method (see details in Supporting Information).<sup>10</sup> The ITO nanoparticles were subsequently dispersed into a TMA/ethanol solution (50 mg/mL) under sonication. The mixture was kept at room temperature for 24 h in a shaking incubator. The ITO nanoparticles were collected after centrifugation and repeated washing with acetonitrile under sonication. The samples were finally dried at room temperature under vacuum.

**Characterization.** Diffuse reflectance infrared Fourier transform spectra were obtained using a Harrick praying mantis accessory incorporated into a Varian Excalibur FTS-3000 FTIR spectrometer. The Fourier transform infrared spectra were collected on a Varian 3100 spectrometer. X-ray photoelectron spectroscopy was recorded on a Kratos AXIS Ultra HAS spectrometer equipped with a monochromatic Al K $\alpha$  X-ray source ( $h\nu = 1486$  eV) operated at 15 kV and 5 mA. Peak fitting was performed with the software XPSPEAK 4.1 and a Shirley background subtraction.

**Electrochemical Measurement.** Cyclic voltammetry of the TMA-modified ITO nanoparticles toward the probe molecules of ferrocene was collected by a standard three-port electrochemical cell and a CHI900B electrochemical workstation. The measurement was performed with an Ag/AgCl reference electrode, a platinum counter electrode, and a gold working electrode covered by the TMA-adsorbed ITO nanoparticles. LiClO<sub>4</sub> (0.25 M) and ferrocene (1 mM) in distilled acetonitrile served as the supporting electrolyte and the electrochemically active probe material, respectively. All data were collected after several scans to achieve good reproducibility with a scan rate of 50 mV/s.

**Computational Details.** First-principles calculations were performed using density functional theory as implemented in the VASP code<sup>11,12</sup> with the electron-ion interactions described by the projector augmented wave (PAW) method.<sup>13,14</sup> The exchange-correlation potential was incorporated in the generalized gradient approximation (GGA) using the Perdew-Burke-Ernzerhof (PBE) functional.<sup>15</sup> All the geometrical structures were fully relaxed until the total energy was converged to be  $<10^{-5}$  eV and the total force  $<0.01$  eV/Å on each atom. A cutoff energy of 500 eV was used.

The as-prepared ITO nanocrystals show the bixbyite crystal structure (body-centered cubic, space group:  $Ia\bar{3}$ ), as confirmed by the X-ray diffraction pattern (Supporting Information Figure S1). The bixbyite crystal structure was used throughout the computation. The (111) surface of bixbyite In<sub>2</sub>O<sub>3</sub> is featured by the O-In-O unit, named as a trilayer structure. Here, the ITO (111) surface model includes two trilayers, containing 30 In, 48 O, and 2 Sn atoms and representing 6.25 at % dopant ratio.

During the structural optimization, the bottom O-In-O layer was fixed. A vacuum of 25 Å was inserted between adjacent slabs to prevent artificial interslab interactions. A mesh of  $9 \times 9 \times 1$  Monkhorst-Pack<sup>16</sup>  $k$ -points was used for the total energy calculation.

To evaluate the total energy variation of different adsorption configurations, we define the dissociative chemisorption energy ( $\Delta E$ ) by

$$\Delta E = E_{\text{TMA+surface}} - E_{\text{TMA}} - E_{\text{surface}}$$

where  $E_{\text{TMA+surface}}$ ,  $E_{\text{TMA}}$ , and  $E_{\text{surface}}$  refer to the total energies of the relaxed TMA-adsorbed surface slab, the relaxed free TMA molecule, and the optimized clean surface, respectively.

## ■ RESULTS AND DISCUSSION

**Diffuse Reflectance Infrared Fourier Transform Spectroscopy.** The as-prepared ITO nanocrystals are in a body-centered cubic crystal structure with a spherical shape and an average size of about 10 nm (Figures S1 and S2 in Supporting Information). The diffuse reflectance infrared Fourier transform (DRIFT) spectra of the ITO nanoparticles before and after modification by trimesic acid are shown in Figure 1a,b,

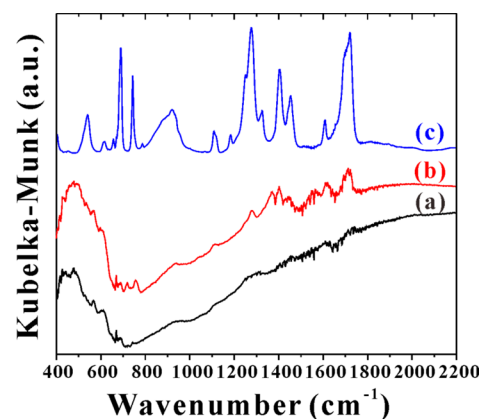


**Figure 1.** DRIFT spectra of (a) bare ITO, (b) TMA-modified ITO nanoparticles, and (c) solid TMA.

respectively. The DRIFT spectrum of pure TMA is also presented as a reference (Figure 1c). It is clearly shown that several new absorption bands appear at 1714, 1616, 1567, 1450, 1370, and 1280  $\text{cm}^{-1}$  for the TMA-modified ITO nanoparticles. The appropriate assignments have been tabulated in Table S1 in Supporting Information, according to the reported works.<sup>17–22</sup> Comparing the three spectra, we can easily discern the two new bands at 1370 and 1567  $\text{cm}^{-1}$ , respectively, which are ascribed to the typical symmetric ( $\nu_s$ ) and asymmetric ( $\nu_{as}$ ) stretching modes of  $\text{COO}^-$ .

**Transmission Fourier Transform Infrared Spectroscopy (FTIR).** Due to the strong absorption of water vapor in the DRIFT spectrum, transmission FTIR was used to further study the surface modification of ITO nanocrystals by trimesic acid. Figure 2 shows the FTIR spectra of the bare ITO nanoparticles, TMA-adsorbed ITO nanoparticles, and pure solid TMA. As shown in Figure 2b, the TMA-modified ITO nanoparticles display several new absorption bands at 1567, 1439, and 1370  $\text{cm}^{-1}$ , compared with the bare ITO nanoparticles. The corresponding assignments are also listed in Supporting Information Table S1. Obviously, the two new absorption bands at 1370 and 1567  $\text{cm}^{-1}$  are in good agreement with the

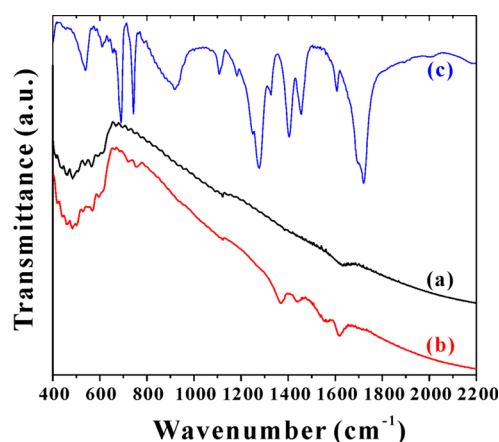


**Figure 2.** FTIR spectra of (a) bare ITO, (b) TMA-adsorbed ITO nanoparticles, and (c) solid TMA.

DRIFT spectrum, suggesting the formation of carboxylate species upon modification of ITO nanoparticles by TMA. The band peaking at  $1628\text{ cm}^{-1}$  for ITO nanoparticles prior to the surface modification is attributed to the scissoring mode of adsorbed water molecules.<sup>23</sup>

**X-ray Photoelectron Spectroscopy (XPS).** The formation of surface carboxylate species can be further consolidated by the C 1s XPS spectra. Figure 3 depicts the C 1s core-level

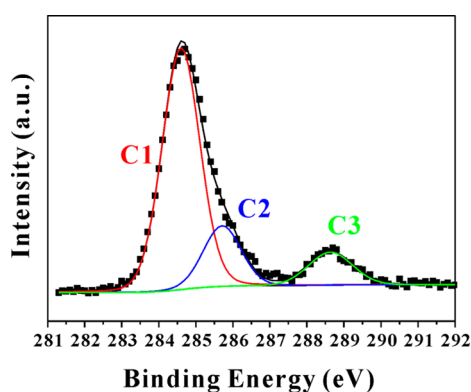


**Figure 3.** C 1s core-level XPS spectrum of the TMA-modified ITO nanoparticles.

spectrum of ITO nanoparticles upon adsorption of TMA. The peak can be fitted into three species, C1, C2, and C3, respectively. The first two are ascribed to the aliphatic carbon ( $284.6\text{ eV}$ ) and C–O related carbon ( $285.7\text{ eV}$ ), respectively, which can be frequently observed on metal oxides. However, the C3 component sitting at the high binding energy of  $288.6\text{ eV}$  clearly indicates the existence of carboxylate or carbonyl carbon on ITO surfaces.<sup>20,24</sup> In contrast, the ITO nanoparticles without surface modification do not show any observable high binding energy peak (Figure S3 in Supporting Information).

**Adsorption of TMA on ITO (111) Surface.** The spectroscopic results shown above convincingly indicate that trimesic acid molecules are successfully attached onto ITO nanocrystals to form carboxylates. However, these spectra do not provide detailed atomistic details on the adsorption behaviors and chemical bonding of TMA with ITO substrate. To gain further insight into the interfacial interactions, we used density functional theory to study the adsorption of TMA on an ITO surface.

The (111) surface of body-centered cubic bixbyite indium oxide nanoparticles was found to be the most preferred orientation (ICDD card no. 06-0416). The stoichiometric (111) surface is essentially nonpolar, resulting from the featured repeating layer of O–In–O along the  $\langle 111 \rangle$  direction. This surface displays the lowest surface energy among the three low-index surfaces in the order of  $\gamma(100) > \gamma(110) > \gamma(111)$ .<sup>25–29</sup> This preferred orientation is also confirmed by the XRD pattern (Figure S1 in Supporting Information). Therefore, the surface was chosen for study of surface chemistry on surface modification by trimesic acid.

Compared with the bulk structure, the coordination numbers of indium and oxygen atoms on the ITO (111) surface are reduced from six to five and four to three, respectively (Figure S4 in Supporting Information). We first systematically sampled possible positions of the dopants in the surface slab. It was identified that the two Sn atoms prefer to be doped with one in each trilayer. The optimized ITO (111) surface is shown in Figure S4a,b in Supporting Information. On the surface trilayer, the replacement of an In atom by a Sn atom is more likely to occur at the six-coordination position on the basis of thermodynamic preference. The doping of the two Sn atoms both in the same trilayer or one in each trilayer but in the positions different from that in Supporting Information Figure S4 results in a total energy of at least  $0.4\text{ eV}$  higher. The top trilayer of the ITO (111) surface slab is depicted in Figure 4

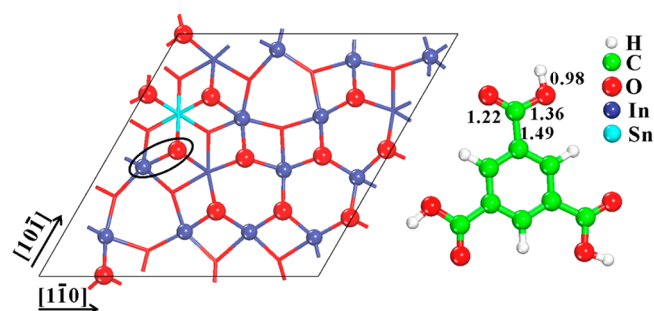


**Figure 4.** ITO (111) surface model (left) and optimized structure of trimesic acid (right). The undercoordinated atoms are shown in balls in the surface model. The ellipse indicates the most preferred adsorption site. The bond lengths are labeled in the unit of Å.

(left), which clearly displays the undercoordinated In and O atoms on the surface. The selected unit cell of the stoichiometric ITO (111) surface provides 12 five-coordination indium and 12 three-coordination oxygen atoms for the adsorption of trimesic acid.

The free TMA molecule has a planar structure arising from the extensive  $\pi$ -conjugation with all the three carboxylic groups and the benzene ring (Figure 4, right). Numerous possible adsorption configurations of TMA on the ITO (111) surface were computationally sampled upon geometrical optimization and the vertical adsorption structure was found to be energetically preferred. Figure 5 depicts the optimized lowest-energy adsorption configuration (the adsorption site indicated by the ellipse in Figure 4). The computational results suggest that the TMA molecule undergoes a quasidissociative chemisorption process to form a carboxylate species on the ITO (111) surface. The  $\pi$ -conjugation remains essentially intact upon surface adsorption except with a partially broken O–H bond, as clearly shown in Figure 5. The dissociative chemisorption is driven by the strong H-bonding interaction



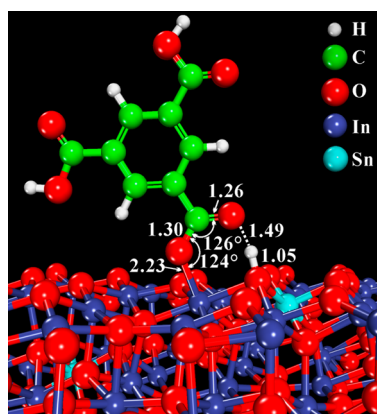


**Figure 5.** Perspective view of the most stable adsorption configuration of TMA on the ITO (111) surface. The bond lengths are labeled in the unit of Å.

between the H atom of a carboxylic group of TMA and the nearby surface O atom and the formation of a covalent O–In bond between the carboxylic group and surface. The benzene ring of the adsorbed TMA molecule is tilted slightly away from the surface normal. The dissociative chemisorption process is essentially spontaneous with virtually no activation barrier (Figure S5 in Supporting Information). The calculated chemisorption energy is  $-1.42$  eV. The results indicate that direct modification of ITO nanoparticle surfaces with TMA is thermodynamically favorable and kinetically facile. The results are consistent with the experimental observations. The geometrical parameters and dissociative chemisorption energies of other possible adsorption configurations are shown in Table S2 in Supporting Information. TMA molecules show similarly vertical adsorption configurations on ITO (111) surface with the highest chemisorption energy of  $-0.83$  eV. The computational results indicate that the TMA molecule prefers to be adsorbed in a vertical adsorption geometry on ITO (111) surface. The adsorbed molecule may act as a bridge for electron transport between ITO and organic layer in electronic devices.

**Cyclic Voltammetry (CV).** The electrochemical performance of the TMA-modified ITO nanocrystals was tested by cyclic voltammetry (CV) to examine the surface reactivity toward the probe molecule, ferrocene (Fc). Figure 6 shows the CV behavior of  $\text{Fc}/\text{Fc}^+$  on a Au electrode covered by ITO nanoparticles. Obviously, the TMA-modified ITO nanocrystals exhibit substantially enhanced peak currents by more than 6-fold. The results suggest that the adsorbed TMA molecules are

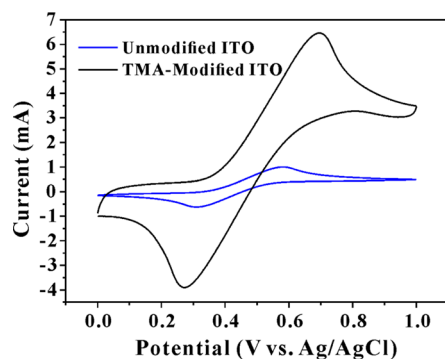


**Figure 6.** Normalized cyclic voltammograms of different electrode materials toward the redox reactions of 1 mM  $\text{Fc}/\text{Fc}^+$  in  $\text{CH}_3\text{CN}$ .

capable of effectively raising the charge-transfer rate and thus substantially boosting the electrocatalytic effect.<sup>6,7</sup>

The significant enhancement of electron transfer can be explained on the basis of the  $\pi$ – $\pi$  interaction between ferrocene and the adsorbed TMA molecule. The vertical adsorption structure of TMA on the ITO nanocrystal surface can facilitate electron transfer first between ferrocene and TMA via a  $\pi$ -stacked electron hopping mechanism and then through the interfacial bonding between TMA and the electrical conductor of ITO, as schematically illustrated in Figure 7.

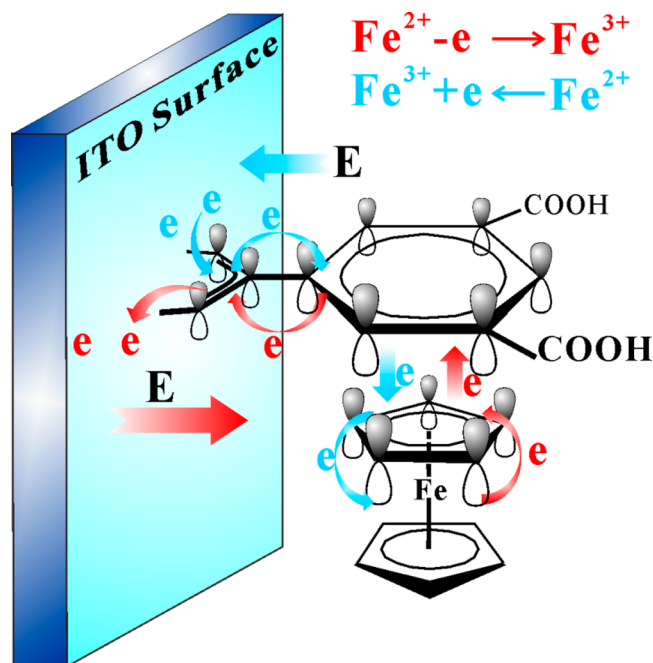


**Figure 7.** Schematic illustration of the enhanced electron transfer process. The electron transfer during the redox process of Fc is illustrated in red (oxidation) and cyan (reduction). E points to the corresponding direction of an electrical field.

The role of TMA is to mediate the electron transfer via its extensive  $\pi$ -conjugation and strong covalent bonding with the ITO nanoparticle surface, leading to a facile redox process for the electrochemical catalytic reaction. Electron transport between  $\pi$ -stacked aromatic systems has been observed in many studies.<sup>30–32</sup> The modification of ITO surfaces with trimesic acid may find applications in organic light-emitting devices and organic photovoltaics, where rapid charge transfer through interfaces is highly desired.<sup>4,6,7</sup>

## CONCLUSIONS

We have used an extensively  $\pi$ -conjugated aromatic molecule TMA to modify ITO nanoparticle surfaces through a dissociative chemisorption. The surface chemistry was characterized by DRIFT, FTIR, and XPS spectroscopic techniques. The results indicate that TMA molecules are adsorbed on ITO nanoparticles, leading to the formation of carboxylate species. DFT computations reveal that the TMA molecule prefers an upstanding configuration on the ITO (111) surface to form a surface species, in good agreement with the experimental observations. The dissociative chemisorption was found to occur spontaneously upon contact of the TMA molecule with the ITO (111) surface with a highly exothermic thermochemical energy. The process is dictated by the formation of a strong

covalent O–In bond between the carboxylate species of TMA and the ITO surface and the hydrogen bonding interaction of the carboxylate species with the nearest O atom in the proximity of the adsorption site. The upstanding adsorption configuration of the extensively  $\pi$ -conjugated TMA on an electrically conductive ITO nanoparticle offers a favorable interaction configuration for molecules participating in a redox reaction. Indeed, the TMA-modified ITO nanoparticles display a substantially enhanced electrocatalytic capability toward ferrocene via an electron transfer mechanism enabled by the  $\pi$ – $\pi$  stacking between ferrocene and the adsorbed TMA molecules and by the strong covalent bond between the carboxylate species and the ITO surface. The ability to facilitate rapid charge transfer through interfaces enabled by ITO surface modifications with judiciously selected organic molecules is important for applications in optoelectronics.

## ■ ASSOCIATED CONTENT

### ■ Supporting Information

Synthesis and characterization of ITO nanocrystals, the assignments of DRIFT and FTIR absorption bands, C 1s XPS of ITO nanoparticles before surface modification, ITO (111) surface slab model, geometries of 24 possible adsorption configurations, and the total energy variation of the lowest-energy adsorption configuration during geometrical optimization. This material is available free of charge via the Internet at <http://pubs.acs.org>.

## ■ AUTHOR INFORMATION

### Corresponding Authors

\*E-mail: [chmxugq@nus.edu.sg](mailto:chmxugq@nus.edu.sg).

\*E-mail: [chmch@nus.edu.sg](mailto:chmch@nus.edu.sg).

### Notes

The authors declare no competing financial interest.

## ■ ACKNOWLEDGMENTS

The authors gratefully acknowledge the support of a start-up grant from National University of Singapore, a FRC Tier 1 grant from Singapore Ministry of Education, a POC grant from National Research Foundation of Singapore, and a DSTA grant and the National Natural Science Foundation of China (No. 21233006).

## ■ REFERENCES

- (1) Pasquarelli, R. M.; Ginley, D. S.; O'Hayre, R. Solution Processing of Transparent Conductors: From Flask to Film. *Chem. Soc. Rev.* **2011**, *40*, 5406–5441.
- (2) Chen, Z.; Li, W.; Li, R.; Zhang, Y.; Xu, G.; Cheng, H. Fabrication of Highly Transparent and Conductive Indium-Tin Oxide Thin Films with a High Figure of Merit via Solution Processing. *Langmuir* **2013**, *29*, 13836–13842.
- (3) Armstrong, N. R.; Veneman, P. A.; Ratcliff, E.; Placencia, D.; Brumbach, M. Oxide Contacts in Organic Photovoltaics: Characterization and Control of Near-Surface Composition in Indium-Tin Oxide (ITO) Electrodes. *Acc. Chem. Res.* **2009**, *42*, 1748–1757.
- (4) Armstrong, N. R.; Carter, C.; Donley, C.; Simmonds, A.; Lee, P.; Brumbach, M.; Kippelen, B.; Domercq, B.; Yoo, S. Interface Modification of ITO Thin Films: Organic Photovoltaic Cells. *Thin Solid Films* **2003**, *445*, 342–352.
- (5) Hotchkiss, P. J.; Jones, S. C.; Paniagua, S. A.; Sharma, A.; Kippelen, B.; Armstrong, N. R.; Marder, S. R. The Modification of Indium Tin Oxide with Phosphonic Acids: Mechanism of Binding, Tuning of Surface Properties, and Potential for Use in Organic Electronic Applications. *Acc. Chem. Res.* **2012**, *45*, 337–346.
- (6) Carter, C.; Brumbach, M.; Donley, C.; Hreha, R. D.; Marder, S. R.; Domercq, B.; Yoo, S.; Kippelen, B.; Armstrong, N. R. Small Molecule Chemisorption on Indium-Tin Oxide Surfaces: Enhancing Probe Molecule Electron-Transfer Rates and the Performance of Organic Light-Emitting Diodes. *J. Phys. Chem. B* **2006**, *110*, 25191–25202.
- (7) Donley, C.; Dunphy, D.; Paine, D.; Carter, C.; Nebesny, K.; Lee, P.; Alloway, D.; Armstrong, N. R. Characterization of Indium-Tin Oxide Interfaces using X-Ray Photoelectron Spectroscopy and Redox Processes of a Chemisorbed Probe Molecule: Effect of Surface Pretreatment Conditions. *Langmuir* **2002**, *18*, 450–457.
- (8) Zotti, G.; Schiavon, G.; Zecchin, S.; Berlin, A.; Pagani, G. Adsorption of Ferrocene Compounds on Indium-Tin-Oxide Electrodes. Enhancement of Adsorption by Decomposition of Ferrocenium Molecules by Oxygen. *Langmuir* **1998**, *14*, 1728–1733.
- (9) Lee, J.; Petruska, M. A.; Sun, S. Surface Modification and Assembly of Transparent Indium Tin Oxide Nanocrystals for Enhanced Conductivity. *J. Phys. Chem. C* **2014**, *118*, 12017–12021.
- (10) Goebbert, C.; Nonninger, R.; Aegerter, M. A.; Schmidt, H. Wet Chemical Deposition of ATO and ITO Coatings using Crystalline Nanoparticles Redispersable in Solutions. *Thin Solid Films* **1999**, *351*, 79–84.
- (11) Kresse, G.; Furthmüller, J. Efficiency of Ab-Initio Total Energy Calculations for Metals and Semiconductors using a Plane-Wave Basis Set. *Comput. Mater. Sci.* **1996**, *6*, 15–50.
- (12) Kresse, G.; Furthmüller, J. Efficient Iterative Schemes for Ab-Initio Total-Energy Calculations using a Plane-Wave Basis Set. *Phys. Rev. B* **1996**, *54*, 11169–11186.
- (13) Blochl, P. E. Projector Augmented-Wave Method. *Phys. Rev. B* **1994**, *50*, 17953–17979.
- (14) Kresse, G.; Joubert, D. From Ultrasoft Pseudopotentials to the Projector Augmented-Wave Method. *Phys. Rev. B* **1999**, *59*, 1758–1775.
- (15) Perdew, J. P.; Burke, K.; Ernzerhof, M. Generalized Gradient Approximation Made Simple. *Phys. Rev. Lett.* **1996**, *77*, 3865–3868.
- (16) Monkhorst, H. J.; Pack, J. D. Special Points for Brillouin-Zone Integrations. *Phys. Rev. B* **1976**, *13*, 5188–5192.
- (17) Mayo, D. W. Characteristic Frequencies of Aromatic Compounds (Group Frequencies of Arenes). In *Course Notes on the Interpretation of Infrared and Raman Spectra*; John Wiley & Sons, Inc.: New York, 2004; pp 101–140.
- (18) Arenas, J. F.; Montañez, M. A.; Otero, J. C.; Marcos, J. I. Surface Enhanced Raman Spectra of Benzene Tricarboxylate Anions on Silver Sols. *Vib. Spectrosc.* **1993**, *4*, 159–165.
- (19) Kim, Y.; Cho, K.; Lee, K.; Choo, J.; Gong, M.; Joo, S. Electric Field-Induced Adsorption Change of 1,3,5-Benzenetricarboxylic Acid on Gold, Silver, and Copper Electrode Surfaces Investigated by Surface-Enhanced Raman Scattering. *J. Mol. Struct.* **2008**, *878*, 155–161.
- (20) Classen, T.; Lingenfelder, M.; Wang, Y.; Chopra, R.; Virojanadara, C.; Starke, U.; Costantini, G.; Fratesi, G.; Fabris, S.; Gironcoli, S.; et al. Hydrogen and Coordination Bonding Supramolecular Structures of Trimesic Acid on Cu(110). *J. Phys. Chem. A* **2007**, *111*, 12589–12603.
- (21) Li, Z.; Han, B.; Wan, L. J.; Wandlowski, T. Supramolecular Nanostructures of 1,3,5-Benzene-Tricarboxylic Acid at Electrified Au(111)/0.05 M H<sub>2</sub>SO<sub>4</sub> Interfaces: An in Situ Scanning Tunneling Microscopy Study. *Langmuir* **2005**, *21*, 6915–6928.
- (22) Han, B.; Li, Z.; Wandlowski, T. Adsorption and Self-Assembly of Aromatic Carboxylic Acids on Au/Electrolyte Interfaces. *Anal. Bioanal. Chem.* **2007**, *388*, 121–129.
- (23) Noei, H.; Qiu, H.; Wang, Y.; Löffler, E.; Woll, C.; Muhler, M. The Identification of Hydroxyl Groups on ZnO Nanoparticles by Infrared Spectroscopy. *Phys. Chem. Chem. Phys.* **2008**, *10*, 7092–7097.
- (24) Zhang, W.; Cao, L.; Wan, L.; Liu, L.; Xu, F. A Photoelectron Spectroscopy Study on the Interfacial Chemistry and Electronic Structure of Terephthalic Acid Adsorption on TiO<sub>2</sub>(110)-(1 × 1) Surface. *J. Phys. Chem. C* **2013**, *117*, 21351–21358.

- (25) Pussi, K.; Matilainen, A.; Dhanak, V. R.; Walsh, A.; Egdel, R. G.; Zhang, K. H. L. Surface Structure of  $\text{In}_2\text{O}_3(111)$  ( $1 \times 1$ ) Determined by Density Functional Theory Calculations and Low Energy Electron Diffraction. *Surf. Sci.* **2012**, *606*, 1–6.
- (26) Walsh, A.; Catlow, C. R. A. Structure, Stability and Work Functions of the Low Index Surfaces of Pure Indium Oxide and Sn-Doped Indium Oxide (ITO) from Density Functional Theory. *J. Mater. Chem.* **2010**, *20*, 10438–10444.
- (27) Paramonov, P. B.; Paniagua, S. A.; Hotchkiss, P. J.; Jones, S. C.; Armstrong, N. R.; Marder, S. R.; Brédas, J. L. Theoretical Characterization of the Indium Tin Oxide Surface and of its Binding Sites for Adsorption of Phosphonic Acid Monolayers. *Chem. Mater.* **2008**, *20*, 5131–5133.
- (28) Li, H.; Paramonov, P.; Bredas, J. L. Theoretical Study of the Surface Modification of Indium Tin Oxide with Trifluorophenyl Phosphonic Acid Molecules: Impact of Coverage Density and Binding Geometry. *J. Mater. Chem.* **2010**, *20*, 2630–2637.
- (29) Agoston, P.; Albe, K. Thermodynamic Stability, Stoichiometry, and Electronic Structure of  $\text{bcc-In}_2\text{O}_3$  Surfaces. *Phys. Rev. B* **2011**, *84*, 045311.
- (30) Li, X. C.; Sirringhaus, H.; Garnier, F.; Holmes, A. B.; Moratti, S. C.; Feeder, N.; Clegg, W.; Teat, S. J.; Friend, R. H. A Highly  $\pi$ -Stacked Organic Semiconductor for Thin Film Transistors Based on Fused Thiophenes. *J. Am. Chem. Soc.* **1998**, *120*, 2206–2207.
- (31) Tauber, M. J.; Kelley, R. F.; Giaimo, J. M.; Rybtchinski, B.; Wasielewski, M. R. Electron Hopping in  $\pi$ -Stacked Covalent and Self-Assembled Perylene Diimides Observed by ENDOR Spectroscopy. *J. Am. Chem. Soc.* **2006**, *128*, 1782–1783.
- (32) Solomon, G. C.; Herrmann, C.; Vura-Weis, J.; Wasielewski, M. R.; Ratner, M. A. The Chameleonic Nature of Electron Transport through  $\pi$ -Stacked Systems. *J. Am. Chem. Soc.* **2010**, *132*, 7887–7889.